Talanta 107 (2013) 338–343

Contents lists available at SciVerse ScienceDirect

Talanta

journal homepage: www.elsevier.com/locate/talanta

Model and experimental investigations of aluminum oxide slurry transportation and vaporization behavior for nebulization inductively coupled plasma optical emission spectrometry

Zheng Wang [a,*], Junye Zhang [a], Huijun Zou [a], Min Dong [a], Deren Qiu [b], Pengyuan Yang [b,**]

[a] Shanghai Institute of Ceramics, Chinese Academy of Sciences, Shanghai 200050, China
[b] Department of Chemistry, Fudan University, Shanghai 200433, China

ARTICLE INFO

Article history:
Received 20 October 2012
Received in revised form
15 January 2013
Accepted 17 January 2013
Available online 8 February 2013

Keywords:
Model
Aluminum oxide
Slurry nebulization
Inductively coupled plasma

ABSTRACT

We analyzed aluminum oxide (Al_2O_3) by slurry introduction inductively coupled plasma (ICP) optical emission spectrometry through modeling and experimentation. We also studied the relationship between the ICP nebulizer gas flow, the spray chamber geometry, and the particle size of Al_2O_3 in an attempt to minimize the need for correction factors by ensuring an efficient aerosol mass transport. A cut-off point for the particle size was implemented at approximately 7–10 μm for the sample introduction system. Based on modeling using a customized computer model and some experimental evidences, the maximum particle size for complete vaporization is approximately 7 μm. For a gas flow of 0.8 L min^{-1}, particles with a diameter of up to 8 μm can be evaporated with an efficiency of 68% and particles as large as 5 μm can be evaporated completely within the nebulization gas flow region. The Al_2O_3 sintering block was ground using a self-made alumina mortar combined with a mixer mill device for particle reduction. The sample slurry was prepared by directly dispersing powdered Al_2O_3 in an aqueous solution with an addition of 0.5 wt% poly (acrylate amine) (NH_4PAA) as the dispersant. The accuracy of the results was compared with the data obtained through high-pressure digestion with acid and with the value of a certified reference material, NIST SRM 699 alumina.

© 2013 Elsevier B.V. All rights reserved.

1. Introduction

Slurry introduction combined with inductively coupled plasma optical emission spectrometry or mass spectrometry (ICP-OES/MS) is a feasible way to analyze powdery materials directly. Researchers have verified the effectiveness of the procedure for the analysis of powdery samples such as coal [1,2], geological materials [3,4], cement [5,6], biological materials [7,8] and size-tailored magnetic colloids [9]. This technique can also be used to characterize ceramic powders, which are being developed for numerous applications because of their desirable features. The increasing applications of high-tech ceramic materials in various fields of science and technology indicate that desirable properties of ceramics must be further investigated. These properties are often directly correlated with the contents of trace impurities. The direct analysis of powders by ICP-OES is desirable to avoid contaminations and losses of analytes as well as lengthy procedures associated with digestion. Therefore, powerful, rapid, and reliable analytical methods are required for material characterization. Several papers have reported the use of slurry introduction in ceramic analysis [10–21]. Analytical methods based on slurry introduction have several advantages, namely, ease of use and rapid analysis. However, the complexities of this approach, in which solid samples are directly analyzed in an aqueous slurry of a fine powdery material, are apparent. A highly stable and homogeneous slurry is required for precise and accurate analytical results [22]. In analyzing ceramic materials, the particle size of the starting powders is a critical factor. Many studies have reported that slurry particles larger than 5 μm (in several studies, 2 μm) do not reach the plasma, which results in signal loss [23]. In our previous study, we reported a particle size of titanium nitride powders in the μm level (80% of the powdered particles were less than 10 μm and had a mean diameter of 4.9 μm) by using slurry nebulization ICP for impurity analysis [24]. All analytical results were below the average compared with the results of fusion-prepared samples. Therefore, all sample results were multiplied by a correction factor of five to obtain a semi-quantitative method for rapid screening analysis. When refined aluminum nitride powders were used (most powdered particles were smaller than 7 μm with a mean diameter of 1.9 μm) and with the aid of dispersants, several elements with high boiling points, such as

* Corresponding author. Tel.: +86 2152413503; fax: +86 21 52413016.
** Corresponding author.
E-mail address: wangzheng@mail.sic.ac.cn (Z. Wang).

0039-9140/$ - see front matter © 2013 Elsevier B.V. All rights reserved.
http://dx.doi.org/10.1016/j.talanta.2013.01.045

Si and Y, achieved a signal intensity of only 40–60% compared with equivalent aqueous standards [25].

The strong dependence of recovery on the particle size distribution of the slurry has particular implications for calibration. The use of a slurry standard or empirical correction factors for calibration is risky. Relatively subtle changes in the particle size distribution of the sample slurries are useless to the calibration procedure and can degrade the precision of the analysis [26]. Aqueous standards should be used for calibration to shorten the analysis time in slurry nebulization ICP-OES. This calibration should meet two requirements, namely, the analyte transport of slurry particle and the subsequent vaporization efficiency of that particle must be identical to the nebulization of the simple aqueous solution [10]. When the conditions are not met, the analytical accuracy of slurry nebulization ICP-OES decreases. Many attempts have been made to overcome these problems. Numerous studies have investigated the model transportation and vaporization behavior of aluminum oxide (Al_2O_3) and SiC-slurries that were introduced via pneumatic nebulization [27]. In addition, comparative investigations have described the nebulization of slurries and solutions with a Babington nebulizer by using different gas flows. McCurdy and Fry [28] have experimentally demonstrated that coal particles with sizes of up to 17 μm can still reach the plasma. However, Ebdon and Collier [29] reported that quantitative transportation and atomization of kaolin by slurry nebulization with a Babington nebulizer can only be performed when the maximum particle diameter is smaller than 6–8 μm.

In the current paper, we investigated the behavior of alumina slurry particles in the transportation and vaporization process of suspension nebulization ICP-OES to determine the size requirement of slurry nebulization in ICP. A simple and easy method for grinding Al_2O_3 sintering blocks in our laboratory is presented. The analytical results obtained using slurry nebulization ICP-OES with aqueous standard calibrations are evaluated in comparison with the data obtained by high-pressure digestion with acid in a sealed vessel and with the value of a certified reference material, NIST SRM 699 alumina.

2. Experimental

2.1. Instrumentation

All analyses were performed using a VISTA AX ICP-OES spectrometer with an axially viewed configuration (Varian, USA). The sample introduction system consists of a V-groove nebulizer and a reduced-volume Sturman-Masters Type spray chamber made of polytetrafluorethylene. The operating parameters and the selected analytical lines are listed in Table 1. The prepared sample solution or slurry was introduced by a cross nebulizer with a V-groove and was measured by an axially viewed ICP-OES spectrometer. Mixer mill MM40, which has a grinding jar (tungsten carbide, 25 mL, screw top design) (Retsch GmbH Co.), was used for particle reduction.

2.2. Transport behavior of slurry particles

Researchers have determined the diameters in which a particle can be transported to the plasma [26,27,30–32]. The upper limit of the particle size that can be transported into the plasma torch and the effects related to the transport behavior of particular materials from those caused by vaporization were determined by both the particle size distribution of the original ceramic powders and after the pneumatic nebulization of the slurries. A self-made device shown in Fig. 1 was used to investigate the aerosol produced by pneumatic nebulization of the slurry. The aerosol that left the spray chamber and/or crossed the injector torch was trapped in water and collected by the particle collection device.

Table 1
Instrumentation, operating conditions and selected analytical lines.

Spectral range	167–785 nm		
Viewing	Axial		
RF generator	40 MHz		
Torch	All-quartz		
Injector tube diameter	2.3 mm		
Power	1.25 KW		
Plasma flow	15 L/min		
Auxiliary flow	1.5 L/min		
Nebulizer flow	0.65 L/min		
Sample uptake rate	0.8 mL/min		
Analytical lines			
Element	Spectral line(nm)	Element	Spectral line(nm)
Ca	317.933	Na	589.592
Cr	206.149	Ni	231.604
Cu	324.754	Pb	220.353
Fe	238.204	V	309.310
Ga	294.363	Si	251.611
Li	610.365	Ti	336.122
Mg	285.213	Zn	213.857
Mn	257.610		

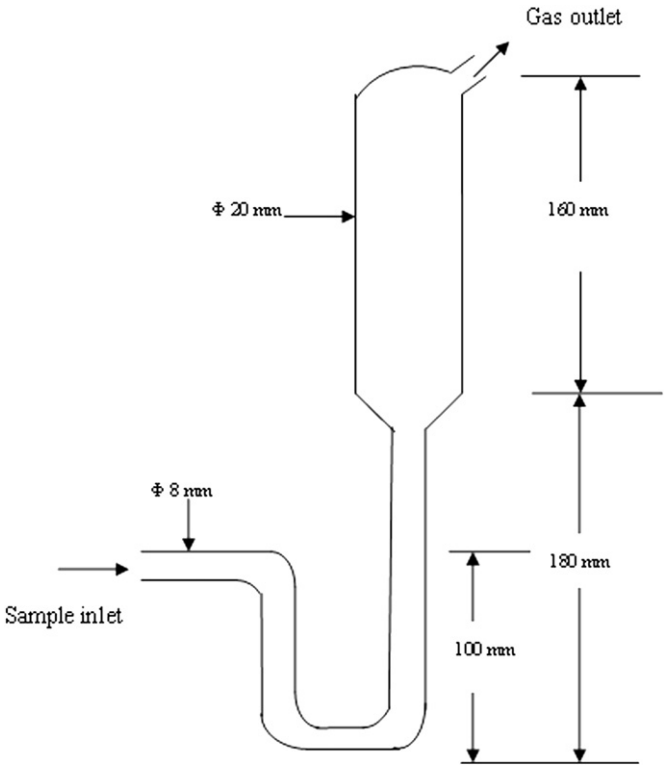

Fig. 1. Particle collection device.

2.3. Vaporization behavior of slurry particles

Al_2O_3 is a material with extreme thermal properties (melting temperature: 2303 K, vaporization temperature: 4548 K) [27,33,34]. On the other hand, the complete vaporization of Al_2O_3 in the plasma is difficult to achieve because of its stability. Thus, a negative deviation occurs when obtaining the results. In this paper, we estimated the vaporization behavior of the slurry particles by using the model developed by Merten and Broekaert as basis [27]. The

upper limit of the particle size that can be completely vaporized in the plasma can be determined by running the computer program. Due to the difference between the conventional side-on viewing and axial viewing, the vaporization rate calculation was changed to calculate the entire torch vaporization processes, while Merten's program calculate the vaporization rate at every view height. Therefore, we added below equation in every repeated iterative operation in the program.

$$\text{Vaporization} = \text{vaporization} + \Delta\text{vaporization}$$

where Δvaporization is the incremental quantity in every repeated iterative operation.

Besides, the influence of the gravitational acceleration was not considerable because the particle move in horizontal and the gravitational acceleration cannot change the orbit of movement of particle in a short time. While in Merten's program the gravitational acceleration was considered because the direction of particle moves is vertical.

2.4. Grinding method

The ceramic particles for slurry preparation must be small enough. Therefore, suitable grinding techniques were employed to reduce the particle size. The material was ground to the desired particle size in our laboratory by the manual comb grinding method by using the mixer mill. A self-made alumina mortar was used to grind the samples. The manufacturing process of the alumina mortar is described as follows: highly pure alumina powders (CR-10, BAIKOWSKI, France), several additives (CMC, dextrin, and PVA), and deionized water were added into the nylon tank and milled for 3 h. The slurry was then sprayed and dried into spherical particles with a size of 50–100 μm. The green body of the crucible was formed by cold isostatic pressing with a pressure of 200 MPa. After removing the binders at 600 °C, the green body was sintered at 1600 °C for 5 h.

2.5. Preparation and characterization of slurries

2.5.1. Reagents and material

All reagents were of guaranteed grade. H_2SO_4 98% was also used in the experiment (Merck, ultrapure). The solutions were prepared using Milli-Q water (18 MΩ cm). The multi-element working standards were prepared from 1000 mg L^{-1} aqueous standards (Shanghai Institute of Measurement and Testing Technology, Shanghai, China).

The two alumina sintering blocks (sintered at 1250 K) were selected for chemical composition analysis. NIST SRM 699 alumina was selected as a certified reference material.

2.5.2. Slurry preparation

The slurry was prepared by weighing an Al_2O_3 sample (1.0 g) and then transferring it into a 100 mL volumetric flask that contains the 0.5 wt% poly (acrylate amine) (NH_4PAA) dispersant (Aldrich Chemical Co., USA). The pH was adjusted to a desired value (6–10) with dilute aqueous hydrochloric acid or dilute aqueous NH_4OH. Before nebulization, the slurry was agitated in an ultrasonic bath for 15 min to keep a stable dispersion.

2.6. High pressure digestion with acid

About 1.00 g of the milled aluminum oxide powder and SRM 699 alumina were accurately weighed and placed in a closed high-pressure PFA decomposition vessel and wet-decomposed. The 15 mL acid mixtures that were used in the decomposition were composed of water and H_2SO_4 98% (3:1). The mixture in the vessel was digested for 16 h at 230 °C. The sample was total dissolution and cooled to room temperature. Then it was transferred into l00 mL polyethylene volume flask with water. The sample was used for comparison with the slurry samples in the analysis.

2.7. Characterization and dispersion of slurries

2.7.1. Zeta potential measurement

The zeta potentials of the slurrys were measured by a Zeta-Plus Analyser (Brookhaven Instruments, USA). The slurrys were prepared by adding different amounts of the dispersant to the Al_2O_3 powders (0.01 wt%). The slurrys were ultrasonically mixed just before the zeta potential was measured.

2.7.2. Size distribution of the sample powder

The particle sizes were determined by SICCAS-4800 Photo-Sedimentometry (Shanghai Institute of Ceramics, CAS).

3. Results and discussion

3.1. Particle size reduction

All large particle samples must undergo particle size reduction before they were dispersed in water. The self-made alumina mortar was used to grind bulk samples. The small bulk or coarse particle powder (appropriately 10.0 g) was then repeatedly milled using the mixer mill. The powder is contained in the shell, and vibrated together with the beads. The grinding material and the particles collided with each other, which results in the breakdown of solid particles. The average diameter decreased to about 0.5 μm after grinding for 3 min (Fig. 2). The particle size was determined by SICCAS-4800 Photo-Sedimentometry. The increased milling time only slightly decreased the average diameter. However, the contamination of elements such as W and Co increased. The changes in the mean particle size with different mill times are shown in Fig. 2. The mean particle size slightly decreased with increasing mill time. The mean particle size showed no significant changes when the milling time was set to more than 2 min. Thus, the mill time was selected as 2 min.

3.2. Aerosol transport loss

Only particles that have sizes smaller than 10 μm have been suggested to contribute to the analyte atomic emission signal [23].

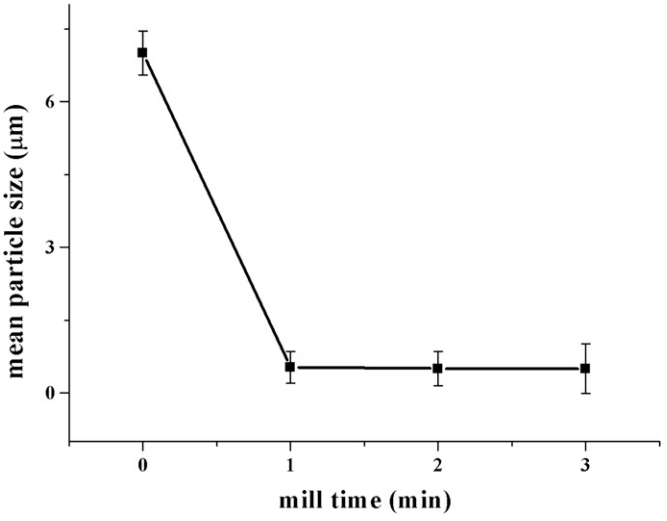

Fig. 2. Relationship between mean particle size and mill time.

The order-sorting of the spray chambers and the gravity effects result in the selective transport of very small particles to the ICP. A coarse aluminum oxide powder sample (Fig. 3) that was screened through a 25 μm (800 meshes) sieve was nebulized to assess if the low recoveries could be directly attributed to the rejection of large particles by the spray chamber. The particles that were dispensed from the spray chamber and the injector tube were collected. The latter represented the case when the sample reached the plasma. The particle size distribution of the Al_2O_3 slurry that was collected from the nebulizer-spray chamber outlet is shown in Fig. 4. The figure clearly shows a cut-off point for the particle size at approximately 7–10 μm. The size distribution of particles that were collected at the torch outlet had no distinct difference from those collected at the spray chamber outlet. The cut-off size was in accordance with our previous results [32], and is also the same with the result reported by Ebdon [35]. Thus, a particle with a size less than 10 μm could reach the plasma. Therefore, according to Fig. 4, the particle size is small enough for slurry preparation.

3.3. Vaporized efficiency and particle size reduce

The vaporization percentage of single Al_2O_3 powders in different particle sizes was calculated using the model developed by Merten and Broekaert to show the effect of particle size on slurry atomization [27]. The relationship between the percentage vaporization of single Al_2O_3 slurry powders and its particle size is shown in Fig. 5. The upper limit of the Al_2O_3 particle size that can be completely vaporized in the plasma is about 7 μm. The vaporization efficiency decreased with increasing particle size, and only about 46% of the particle mass could be vaporized at a particle size of 10 μm.

For analytical applications of slurry nebulization, the vaporation within the nebulizer gas flow is of great importance. By varying the nebulizer gas flow, the residence time of the particles can be influenced. For a gas flow of 0.8 L min^{-1}, particles with a diameter of up to 8 μm can be evaporated with an efficiency of 68% and particles as large as 5 μm can be evaporated completely within the nebulization gas flow region. This is clearly documented by the results of the simulations shown in Fig. 6. The particle must be heated up to its evaporation temperature, which takes a long time for large particles.

For the analysis of advanced ceramic materials by using slurry nebulization ICP-OES with aqueous standard calibrations, an incomplete vaporization caused negative deviations in determining the results. In this paper, efforts were made to reduce the

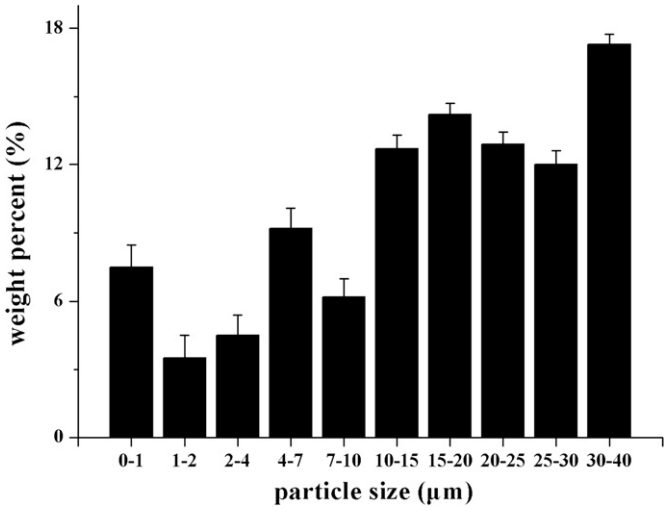

Fig. 3. Bar diagram for particle size distribution of the Al_2O_3 sample screened through a 25 μm (800 meshes) sieve.

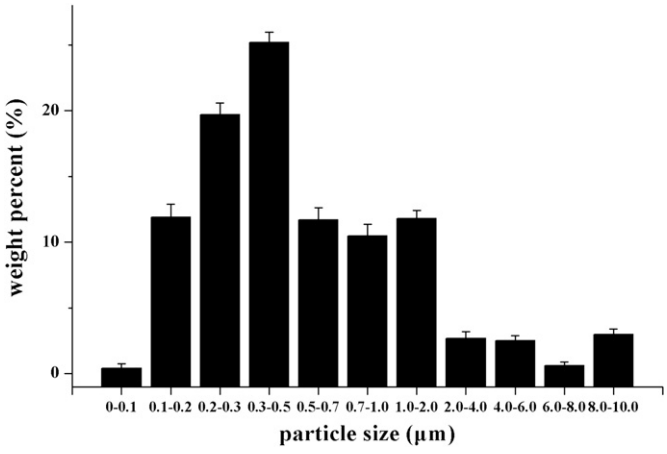

Fig. 4. Bar diagram for Al_2O_3 particle size distributions when passing into the nebulizer-spray chamber.

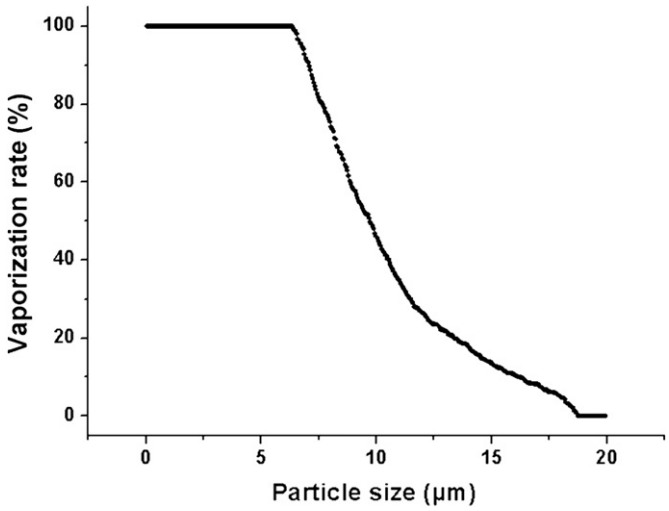

Fig. 5. Relationship between theoretical percentage vaporization of Al_2O_3 and particle size in the case of a nebulizer gas flow of 0.6 L min^{-1}.

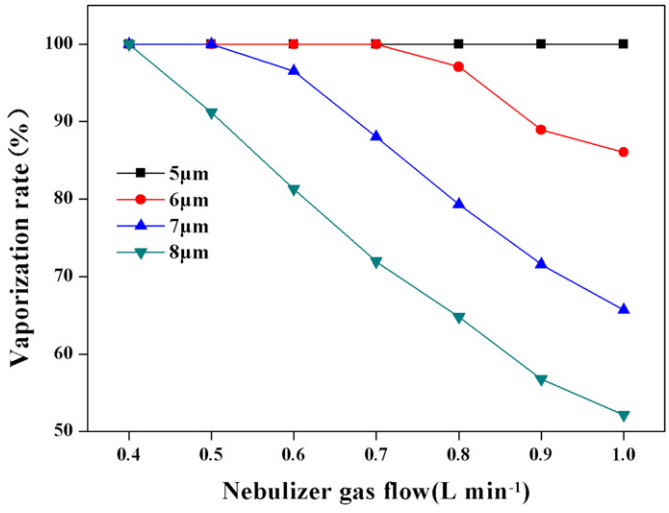

Fig. 6. Calculated evaporation rates for single Al_2O_3 particles in the different nebulization gas flow.

particle size to meet the requirements of slurry nebulization ICP-OES.

3.4. Influence of pH on the slurry

Highly stable and homogeneous slurry is required to produce precise and accurate analytical results. The stability of the suspended slurry is related to the electrostatic interaction between the particles and the nature of the medium, which can be described in terms of the zeta potential of the system. Farinas et al. [36] have discussed the relationship between stability and the zeta potential, and they also investigated the effect of the stability and homogeneity of the slurry on line intensity and measurement precision in ICP-OES. Fig. 7 shows the zeta potential varies with pH at different NH_4PAA concentrations results in different zeta potentials. The isoelectric points (IEP) are found near pH 3.0, whereas a simple aqueous slurry without additive shows the IEP at pH 6.5. The experimental results that the zeta potential at pH 6 drops from about 15 mV for a simple aqueous slurry to about -40 mV for spiked slurries The zeta potentials were appropriately -40 mV in range of pH 6–10, which gives the appropriate pH conditions for slurry preparation. From this Fig. 7, the optimum amount for dispersing the Al_2O_3 powder is 0.5 wt% NH_4PAA, in which zeta potential was constant and have essentially maximum value.

3.5. Calibration and analytical result

The processes of transportation and vaporization are similar for solutions and slurries when the slurry particle size is small enough. Therefore, calibrations with aqueous solutions are possible. In this work, a series of aqueous standards using hydrochloric acid were prepared to establish calibration curves. The analytical result of Al_2O_3 is listed in Table 2. Micro and trace elements in Al_2O_3 were determined using a slurry introduction method, and then compared with the results obtained by acid digestion method. From Table 2, the test results of the two samples that were determined by the slurry introduction method were in good accordance with those of samples prepared via high-pressure acid digestion method. The results of the slurry introduction method for determination of micro and trace elements in NIST standard reference material 699 were in good accordance with the certificate values (Table 3), which confirmed that the calibration curves could be established by aqueous standards if the ceramic particle size is small enough. The repeatability of over 11 slurry measurements was 1–2% for the relative standard deviation of all analytical elements. The LODs expressed in terms of three times of standard deviation (S.D.) of the blanks obtained from a high purity Al_2O_3 slurry are in the range of 0.04–2 μg g^{-1}, superior to those of the acid digestion method and nebulization technique by ICP-OES(0.5–20 μg g^{-1}). The superiority of the slurry nebulization technique is evident: due to the quality control of the water and dispersant during the preparation of the slurry

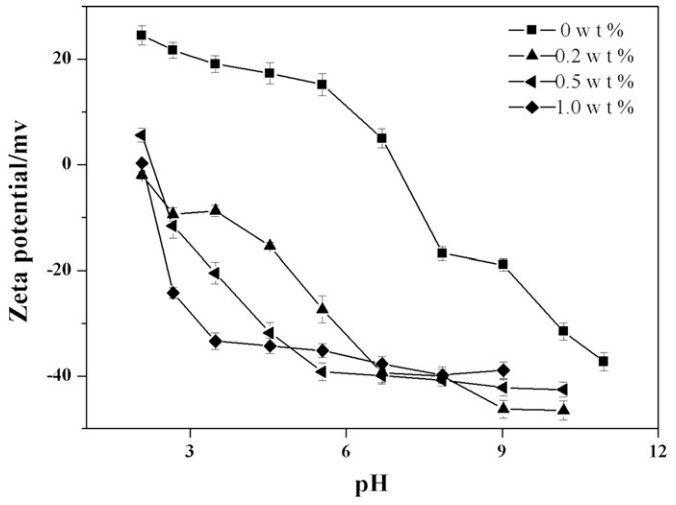

Fig. 7. Profiles of zeta potential versus pH for mm particle sized Al_2O_3 slurry at different NH_4PAA concentrations.

Table 2
Results (μg/g) obtained in the analysis of Al_2O_3 using slurry introduction method using aqueous standard calibration and comparison of high pressure-assisted acid digestion method.

Element	Al_2O_3-I[b]		Al_2O_3-II[b]	
	Slurry introduction method	Acid digestion method	Slurry introduction method	Acid digestion method
CaO	675 ± 30	632 ± 29	11 ± 3	10 ± 2
CuO	61 ± 2	61 ± 3	5 ± 2	4 ± 2
Fe_2O_3	651 ± 25	631 ± 20	12 ± 3	10 ± 3
MgO	45 ± 3	36 ± 6	3 ± 1	–[a]
MnO	54 ± 2	55 ± 3	–[a]	–[a]
Na_2O	120 ± 15	120 ± 10	2 ± 1	–[a]
NiO	30 ± 2	33 ± 3	5 ± 3	5 ± 3
SiO_2	215 ± 16	244 ± 23	18 ± 2	16 ± 3
TiO_2	42 ± 2	43 ± 3	–[a]	–[a]

[a] Not detected.
[b] Mean value ± SD (n=5).

Table 3
Mean value and precision for determination of micro and trace elements in NIST standard reference material 699.

Element	Slurry introduction method[b] (μg/g)	Acid digestion method[b] (μg/g)	Certificate value[b] (μg/g)
CaO	350 ± 18	365 ± 15	360 ± 20
Cr_2O_3	3 ± 1	–[a]	2 ± 1
Fe_2O_3	118 ± 13	125 ± 11	130 ± 10
Ga_2O_3	105 ± 17	102 ± 15	100 ± 20
Li_2O	22 ± 9	17 ± 6	20 ± 10
MgO	7 ± 2	8 ± 2	6 ± 2
MnO	8 ± 3	7 ± 1	5 ± 1
SiO_2	128 ± 10	123 ± 6	120 ± 8
Na_2O	6000 ± 130	5980 ± 120	5900 ± 100
V_2O_3	5 ± 2	6 ± 3	5 ± 2
ZnO	125 ± 16	127 ± 13	130 ± 20

[a] Not detected.
[b] Mean value ± SD (n=5).

4. Conclusion

Particle size distribution constraints on slurry nebulization were routinely performed, i.e., with direct calibration and compared with simple aqueous standards, especially for ceramic materials such as Al_2O_3. The model developed by Merten and Broekaert was modified for the axial configuration of ICP-OES. The results of the experimental and modified model are similar to each other. Based on modeling using a customized computer model and some experimental evidence, the maximum particle size for complete vaporization is approximately 7 μm. Slurry atomization analysis was performed without the aid of matrix matching, standard additions, or correction factors when the particle size is small enough. The method involving the use of simple aqueous standards as calibration samples had the same results as those by the high-pressure-assisted digestion method

and with the value of a certified reference material, NIST SRM 699 alumina.

Acknowledgments

Financial supports from NSFC (20705036), the Plan of Creative funding (SCX0626), and 863 Program (2006AA03Z535) are highly acknowledged.

References

[1] C.J. Walker, D.E. Davey, K.E. Turner, I.C. Hamilton, Fresenius J. Anal. Chem. 355 (1996) 801–802.
[2] L. Ebdon, J.R. Wilkinson, J. Anal. At. Spectrom. 2 (1987) 325–328.
[3] K.E. Jarvis, Chem. Geol. 95 (1992) 73–84.
[4] M. Totland, I. Jarvis, K.E. Jarvis, Chem. Geol. 95 (1992) 35–62.
[5] C.S. Silva, T. Blanco, J.A. Nobrega, Spectrochim. Acta B 57 (2002) 29–33.
[6] L. Marjanovic, R.I. McCrindle, B.M. Botha, H.J. Potgieter, Anal. Bioanal. Chem. 379 (2004) 104–107.
[7] K. Barbro, A. Marit, P. Jean, Talanta 80 (2010) 2068–2075.
[8] L.C. Sola, B.I. Navarro, Food Chem. 115 (2009) 1048–1055.
[9] M.H. Sousa, G.J. da Silva, J. Depeyrot, F.A. Tourinho, L.F. Zara, Microchem. J. 97 (2011) 182–187.
[10] B. Raeymaekers, T. Graule, J.A.C. Broekaert, F. Adams, P. Tschopel, Spectrochim. Acta Part B 43 (1988) 923–940.
[11] T. Graule, A.V. Bohlen, J.A.C. Broekaert, E. Grallath, R. Kloekenkamper, P. Tschopel, G. Tolg, Fresenius J. Anal. Chem. 335 (1989) 637–642.
[12] M. Huang, X. Shen, Spectrochim. Acta Part B 44 (1989) 957–964.
[13] B. Docekal, J.A.C. Broekaert, T. Graule, P. Tsehopel, G. Tolg, Fresenius J. Anal. Chem. 342 (1992) 113–117.
[14] J.A.C. Broekaert, C. Lathen, R. Brandt, C. Pilger, D. Pollmann, P. Tsehopel, G. Tolg, Fresenius J. Anal. Chem. 349 (1994) 20–25.
[15] Z. Wang, D.R. Qiu, G.Y. Tao, P.Y. Yang, J. Anal. At. Spectrom. 24 (2009) 1258–1261.
[16] M.C. Santos, J.A. Nobrega, J. Anal. At. Spectrom. 22 (2007) 93–96.
[17] Z. Wang, J.Y. Zhang, D.R. Qiu, H.J. Zou, H.Y. Qu, Y.R. Chen, P.Y. Yang, J. Anal. At. Spectrom. 25 (2010) 1482–1484.
[18] K. Jankowski, A. Jackowska, P. Lukasiak, M. Mrugalska, A. Trzaskowska, J. Anal. At. Spectrom. 20 (2005) 981–986.
[19] Z. Wang, D.R. Qiu, Z.M. Ni, G.Y. Tao, P.Y. Yang, Anal. Chim. Acta 577 (2006) 288–294.
[20] X.L. Liu, T.C. Duan, Y. Han, X.Y. Jia, W.N. Zhang, H.T. Chen, Chinese J. Anal. Chem. 38 (2010) 693–696.
[21] S.L.C. Ferreira, M. Miró, E.G.P. da Silva, G.D. Matos, P.S. dos Reis, G.C. Brandao, W.N.L. dos. Santos, A.T. Duarte, M.G.R. Vale, R.G.O. Araujo, Appl. Spectrosc. Rev. 45 (2010) 44–46.
[22] Z. Wang, Z.M. Ni, D.R. Qiu, T.Y. Chen, G.Y. Tao, P.Y. Yang, 2004 Winter Conference on Plasma Spectrochemistry, Fort Lauderdale, Florida, TP13.
[23] L. Ebdon, M. Foulkes, K. Sutton, J. Anal. At. Spectrom. 12 (1997) 213–229.
[24] Z. Wang, Z.M. Ni, D.R. Qiu, G.Y. Tao, P.Y. Yang, Spectrochim. Acta Part B 60 (2005) 361–367.
[25] Z. Wang, Z.M. Ni, D.R. Qiu, G.Y. Tao, P.Y. Yang, J. Anal. At. Spectrom. 20 (2005) 315–319.
[26] P. Goodall, M.E. Foulkes, L. Ebdon, Spectrochim. Acta Part B 48 (1993) 1563–1577.
[27] D. Merten, P. Heitland, J.A.C. Broekaert, Spectrochim. Acta Part B 52 (1997) 1905–1922.
[28] D.L. McCurdy, R.C. Fry, Anal. Chem. 58 (1986) 3126–3132.
[29] L. Ebdon, A.R. Collier, Spectrochim. Acta Part B 43 (1988) 355–369.
[30] L. Ebdon, M.E. Foulkes, S. Hill, Microchem. J. 40 (1989) 30–64.
[31] W.A.H. Van Borm, J.A.C. Broekaert, R. Klockenkämper, P. Tschöpel, F.C. Adams, Spectrochim. Acta Part B 46 (1991) 1033–1049.
[32] J.Y. Zhang, Z. Wang, Y.P. Du, D.R. Qiu, P.Y. Yang, Chinese J. Anal. Chem. 39 (2011) 658–663.
[33] I. Barin, Thermochemical Date of Pure Substances, Scientific Press, Beijing, 2003 105–210.
[34] D.L. Ye, Handbook of Thermochemical Date of Inorganic Substances, China, Metallurgical Industry Press, Beijing, 2002 120-121.
[35] S. Sparkes, L. Ebdon, Anal. Proc 23 (1986) 410–412.
[36] J.C. Farinas, R. Moreno, J.M. Mermet, J. Anal. At. Spectrom. 9 (1994) 841–849.